NANO LETTERS

pubs.acs.org/NanoLett

Formation of Wurtzite InP Nanowires Explained by Liquid-Ordering

Rienk E. Algra,[†,‡,§] Vedran Vonk,[§] Didier Wermeille,[∥] Wiesiek J. Szweryn,[§] Marcel A. Verheijen,[‡] Willem J. P. van Enckevort,[§] Arno A. C. Bode,[§] Wim L. Noorduin,[§] Erik Tancini,[∥] Aryan E. F. de Jong,[§] Erik P. A. M. Bakkers,[‡,⊥] and Elias Vlieg*[,§]

[†]Materials innovation institute (M2i), 2628CD Delft, The Netherlands, [‡]Philips Research Laboratories Eindhoven, High Tech Campus 11, 5656AE Eindhoven, The Netherlands, [§]Institute for Molecules and Materials, Radboud University Nijmegen, Heyendaalseweg 135, 6525AJ Nijmegen, The Netherlands, [∥]The European Synchrotron Radiation Facility, BP 220, F-38043, Grenoble Cedex 9, France, and [⊥]Photonics and Semiconductor Nanophysics, Department of Applied Physics, Eindhoven University of Technology, 5600 MB Eindhoven, The Netherlands

ABSTRACT We report an in situ surface X-ray diffraction study of liquid AuIn metal alloys in contact with zinc-blende InP $(111)_B$ substrates at elevated temperatures. We observe strong layering of the liquid metal alloy in the first three atomic layers in contact with the substrate. The first atomic layer of the alloy has a higher indium concentration than in bulk. In addition, in this first layer we find evidence for in-plane ordering at hollow sites, which could sterically hinder nucleation of zinc-blende InP. This can explain the typical formation of the wurtzite crystal structure in InP nanowires grown from AuIn metal particles.

KEYWORDS Nanowires, X-ray diffraction, solid-liquid interface, liquid ordering

Nanowires can be grown from nanosized metal droplets by the vapor−liquid−solid (VLS) growth mechanism, which was first reported by Wagner and Ellis already in 1964.[1] As the name "vapor−liquid−solid" suggests, three phases are involved in this type of nanowire growth.[2] Precursor molecules from the gas phase are decomposed and form an alloy with the metal particle. At the solid−liquid interface, nucleation occurs and the crystalline nanowire grows layer by layer. The crystal structure of nanowires grown by the VLS mechanism is often different from corresponding bulk crystals.[3,4] For instance, intrinsic InP nanowires crystallize in the wurtzite structure, while bulk grown InP crystals have the zinc-blende structure. The different InP crystal structures also result in different photoluminescent properties.[3,1] The metal alloy positioned on top of the nanowires is typical for the VLS growth and has many functions. It has been argued that the shape of the metal particle, and more specifically the contact angle of the droplet with the nanowire side facets, determines the nanowire crystal structure.[3,5] In previous work,[4] we have suggested that not the metal particle shape but the chemical composition and the precise atomic positions at the solid−liquid interface determine the nanowire crystal structure. In this paper, we use surface X-ray diffraction (SXRD) in order to solve in situ the atomic structure at the liquid−solid interface of an AuIn alloy in contact with a $(111)_B$ InP bulk crystal surface at elevated temperatures, simulating the solid−liquid interface during InP nanowire growth from an initial Au particle.[6]

A closely related issue that we will address in this paper is on the physical state of the alloy particle during nanowire growth. Nanowires are often grown below the eutectic temperature of the specific alloy. Several studies have shown that the particle is in the solid state during growth,[7] whereas others have shown that the growth rate is much lower for solid than for liquid particles.[8] We show by using SXRD that while the bulk of the alloy layer is in the liquid phase, the first three layers closest to the InP substrate are layered in the substrate normal direction, suggesting a "quasi-liquid" interface layer. The first layer, in direct contact with the substrate, is enriched with In atoms and shows in-plane ordering. The In atoms preferably occupy hollow sites, which leads to the formation of the wurtzite InP crystal structure.

Studying the solid−liquid interface of genuine nanowires in situ encounters two major problems. First, the actual area covered by nanowires is quite small and second, it requires growth conditions with highly toxic precursor gases. We therefore use a thin alloy film in contact with an InP $(111)_B$ substrate as a model system. The samples consist of triangular pieces with 5−8 mm sides of a $[111]_B$ oriented zinc-blende InP wafer. Here the terminology "B" stands for a phosphor-terminated surface. The substrate is covered by a 100 nm metal layer, which is obtained by simultaneous evaporation of Au and In, resulting in a binary composition with a ratio of 60:40, which was verified with EDX (energy dispersive X-ray) in an SEM (scanning electron microscope).

* To whom correspondence should be addressed. E-mail: e.vlieg@science.ru.nl.
Received for review: 07/9/2010
Published on Web: 12/20/2010

DOI: 10.1021/nl1023996 | *Nano Lett.* **2011,** *11,* 44–48

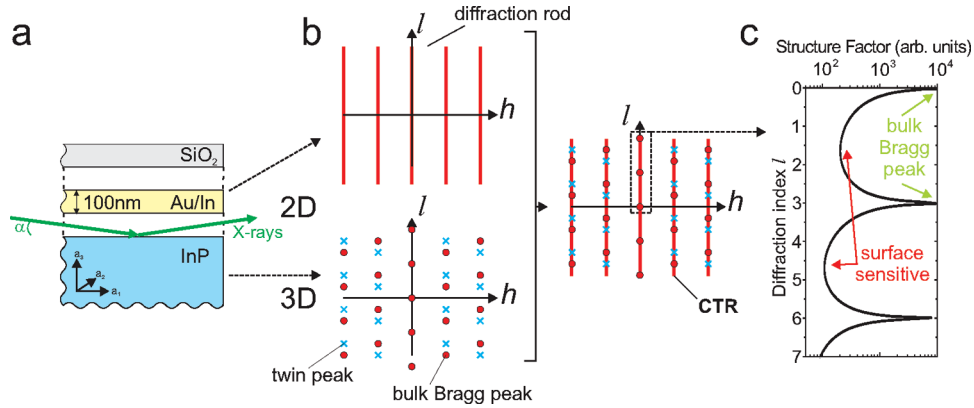

FIGURE 1. Surface X-ray diffraction. (a) A schematic representation of the sample layout. A $[111]_B$ oriented zinc-blende InP wafer is used, followed by a 100 nm thick layer of simultaneously evaporated Au/In alloy (60:40). The metal layer is covered by a SiO_2 layer of 100 nm to minimize decomposition of the InP by evaporation of phosphor. The scattering geometry during SXRD measurements was typically in grazing incidence mode, indicated by the angle α. (b) Diffraction pattern in reciprocal space for a 2D layer resulting in "diffraction rods" (top) and for a 3D bulk crystal resulting in "Bragg peaks" (bottom, red dots). The twin peaks are shown as blue crosses, which are the mirror positions of the Bragg peaks around *l*. If the solid−liquid interface is probed by X-rays, the combination results in CTRs. (c) A CTR gives surface sensitive information in between the bulk Bragg peaks.

This ratio corresponds to the eutectic composition of the AuIn alloy (ϕ phase) at a temperature of 727 K.[9]

The sample layout is shown in Figure 1a. The SXRD experiments are performed in a vacuum chamber (10^{-5} mbar) thus without a PH_3 background pressure. To minimize the decomposition of the InP substrate by phosphor desorption during heating, a 100 nm SiO_2 layer was deposited on top as a diffusion barrier. The samples are resistively heated to 773 K to liquefy the AuIn alloy, similar to the annealing steps prior to nanowire growth. Next, the samples were cooled down to 693 K, a typical growth temperature for InP nanowire growth.[4,10,11] Although this is below the eutectic temperature of the ϕ phase, nanowires are grown at these temperatures with a typical rate of several nm/sec, indicating that the particles are in the liquid state.[4,11−16]

The X-rays probe the periodicity of the bulk InP crystal (3D) and give rise to Bragg peaks in reciprocal space, Figure 1b, at integer diffraction indices (*hkl*). A perfect 2D layer, on the other hand, has no periodicity in the normal direction and therefore diffraction occurs along rods in reciprocal space for all *l* values. The combined diffraction from the two-dimensional (2D) layer and 3D bulk crystal is called a crystal truncation rod (CTR).[17] By measuring the scattered intensities along the CTRs, the amplitude of the structure factors (Fourier transform of the electron density of the unit cell) can be found, see Figure 1c. From these structure factors, the atomic positions and electron density of the interfacial atoms can be derived. The surface sensitive information thus can be found in the CTRs in between the bulk Bragg peaks, as indicated in Figure 1c.

The SXRD experiments were performed at the ID03 beamline[18,19] of the European Synchrotron Radiation Facility (ESRF), Grenoble, using an X-ray energy of 27.5 keV. At the solid−liquid interface, it is expected that the atomic ordering decreases from being completely ordered in the substrate to completely disordered in the liquid. The technique of SXRD is only sensitive to the ordered part of the interface and gives information about the gradual decrease of atomic ordering in the *z*-direction,[20] which is perpendicular to the surface. To describe our results, we use a surface unit cell, which is defined in terms of the InP bulk cubic unit cell as $a_1 = 1/2[1\bar{1}0]$, $a_2 = 1/2[\bar{1}10]$, and $a_3 = [111]$. According to convention, *h* and *k* lie in the surface plane and *l* is along the surface normal. The integrated intensity of different (*hkl*) reflections is determined from rocking scans. After applying the appropriate correction factors,[21] structure factor amplitudes are derived. We used the ANA-ROD package[22] to analyze the data.

At 693 K the specular (0,0,*l*) and the in-plane (1,0,*l*) rods were measured as shown in Figure 2. At room temperature, the (0,0,*l*) rod shows powder diffraction peaks from the solid metal alloy film. The absence of these peaks at 693 K proves that the alloy is liquid at this temperature. The specular (0,0,*l*) rod contains information about the atomic ordering in the *z*-direction. At $l = 4.3$, the data reveals a broad peak (red triangles), which is absent in bulk terminated InP (solid black line). To describe the solid−liquid interface, a model was used consisting of a liquid of *n* atomic layers with a constant spacing and an offset with respect to the substrate surface (Figure 3a). Each layer, having the composition of the ϕ phase, has an occupancy and an anisotropic Debye−Waller factor to define the degree of ordering. The test model uses a phosphor-terminated zinc-blende structure to model the crystalline InP at the interface. More refined modeling with varying spacings and atom types did not give an improved fit, hence this simple model is sufficient to describe the current experimental data.

Fitting of the model to the (0,0,*l*) rod confirms the layering in the *z*-direction; three layers show a strong perpendicular order, and only a little order in the fourth layer. Subsequent layers are invisible and thus have a bulk liquid structure. The fit is shown in Figure 2a, the corresponding structure in

DOI: 10.1021/nl1023996 | *Nano Lett.* **2011,** *11,* 44–48

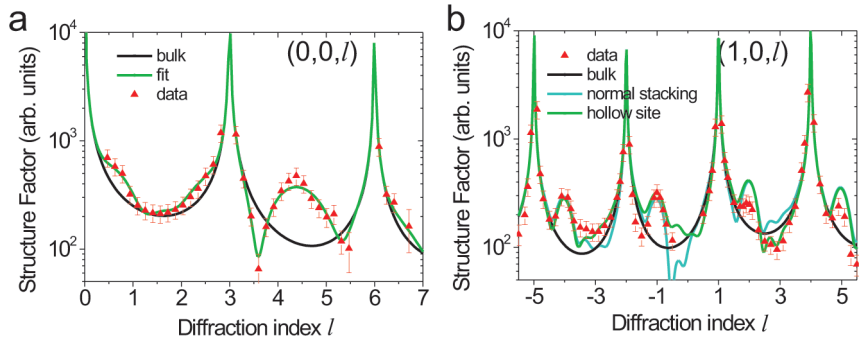

FIGURE 2. Experimental structure factors. Experimental structure factors (red triangles) derived from measured scattered intensities along the (a) (0,0,*l*) rod and (b) (1,0,*l*) rod of the $\{111\}_B$ InP−AuIn solid−liquid interface at a temperature of 693 K. The solid black lines represent the calculated CTRs of a bulk-terminated InP crystal. The blue and green curves represent a normal (continuing the bulk structure) and a hollow-site stacking for the first liquid layer, respectively.

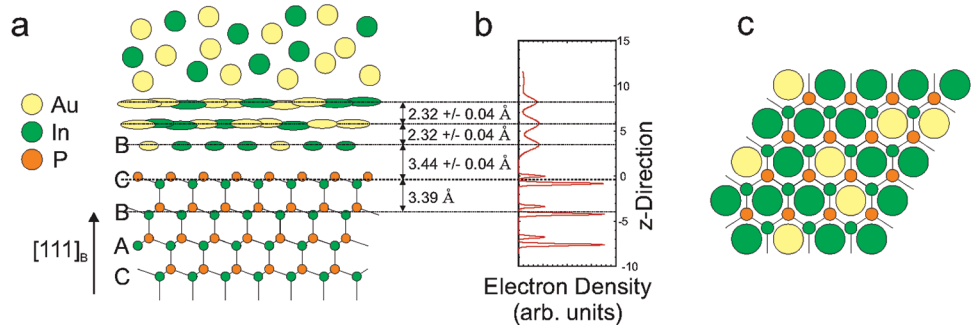

FIGURE 3. Layering (a) schematic atomic structure of the solid−liquid interface accompanied by the corresponding *z*-projected electron density distribution (b). The different atoms are represented in green (In), orange (P), and yellow (Au). The elliptic shapes symbolize the anisotropic in- and out-of-plane liquid ordering whereas the bulk liquid is characterized by larger spheres. (c) Top-view image of the stacking of the first liquid layer on top of a zinc-blende ABC bulk InP structure, indicating that the atoms are positioned in the center of the hexagonal InP rings. The larger spheres represent the in-plane ordering of the atoms in the first liquid layer. The accompanying Debye−Waller parameters are given in Figure 4.

	Au:In ratio	Occupancy	DW in-plane (Å^2)	DW out-plane (Å^2)	Spacing (Å)
Layer 1	60:40 30:70	0.86 +/- 0.09 1.00	70 +/- 10	30 +/- 10	3.44 +/- 0.04
Layer 2	60:40	0.99 +/- 0.07	∞	30 +/- 10	2.32 +/- 0.04
Layer 3	60:40	0.65 +/- 0.07	∞	30 +/- 10	2.32 +/- 0.04
Layer 4	60:40	0.75 +/- 0.13	∞	180 +/- 40	2.32 +/- 0.04

FIGURE 4. Fit parameters. The optimum in- and out-of plane fit parameters are given for each ordered layer, starting with the layer closest to the substrate. The occupancies of ordered atoms in the ϕ phase (60:40 AuIn) are given and the degree of ordering is shown by the Debye−Waller parameters. The spacing is defined as the distance between two successive layers in the liquid alloy. For layer 1, also the composition corresponding to an occupancy of 1 is shown.

Figure 3a. The first layer is positioned at 3.44 ± 0.04 Å from the InP surface, close to the position where the next In-layer of the bulk InP is expected. We find that the spacing between subsequent layers is 2.32 ± 0.04 Å.

The first atomic layer in the liquid is expected to be ordered the most due to the interaction with the substrate. Each next layer is expected to be less ordered, which would result in a decrease of the occupancies of the ordered positions with each next layer and thus in a decrease in the measured electron density. However, from the fit results it can be seen that the electron densities (see Figure 3b) are almost equal for the first three layers. Because of the large correlation between the Debye−Waller and occupancy parameter, the occupancy of the fourth layer seems somewhat high, but within the error bars is equal to the third layer.

This observed layering is rather uncommon compared to other solid−liquid interfaces reported in the literature, where normally the ordering decreases exponentially after the first layer.[20,23−26] The fact that here the first three layers show an equal electron density suggests an unusual step function after three layers. Simulations of exponential segregation and ordering profiles (not shown here) lead to a specular rod profile without any signs of the finite thickness oscillations, that are visible in the data at the fringes for *l* values around 0.8 and 2.2 in Figure 2a. Such oscillations are characteristic for density profiles that contain abrupt steps. Therefore, the density and/or segregation profile at the present interface must contain an abrupt decrease after three atomic layers. It should be realized that the system is thermodynamically very close to an ordered solid phase (ϕ phase),[9] which could induce the observed strong layering. The three layers are

DOI: 10.1021/nl1023996 | *Nano Lett.* **2011,** *11,* 44–48

quasi-liquid and not solid, because that would result in much lower Debye−Waller parameters.[27]

Concerning the composition of these layers are the following. With X-rays, only the electron densities are probed, which makes it difficult to distinguish between different types of atoms. Indeed, using models with layers of pure Au, In or combinations of these atoms always resulted in the same electron density profiles. Nevertheless, the positions of these atomic layers are very accurately determined and can be compared with possible compositions. The spacing of 2.32 Å in the quasi-liquid layer matches d_{110} of bulk In, d_{111} of Au and d_{102} of the ϕ phase, suggesting that all the corresponding layer compositions are plausible. Bulk InP does not have interlayer spacings of 2.32 A and can therefore be ruled out. From a chemical point of view, it is hard to imagine how phosphorus would fit in this quasi-liquid structure, since its presence apparently enlarges the interatomic distances. Furthermore, based on the phase diagrams, which indicate a very low solubility for phosphorus, one would expect phosphorus to either disappear completely from the liquid, or recrystallize into InP. These arguments, together with the in-plane ordering, as discussed further on, leads to the assumption that only Au and In are present in these quasi-liquid layers. Figure 4 lists the parameters assuming the layers have a 60:40 Au−In composition. With this composition, the occupancy of the first layer is found to be lower than the second one, which is highly unlikely. If the first layer is enriched with In, a lighter element than Au, the fitted occupancy increases. The best fit, with a reasonable occupancy of 1, was found with a Au−In ratio of 30:70. This would mean that the interface is enriched with In. It is known that the surface tension of liquid In is a factor 2 lower[28] than that of Au.[29] It is plausible that also at the present solid−liquid interface the interface free energy of In will be lower than that of Au, the more so since the substrate itself contains In and the first alloy layer is positioned at the next InP bulk position. These arguments signify an In-rich solid−liquid interface, containing at least 70% In in the first layer.

The (1,0,*l*) rod, shown in Figure 2b, contains information about in-plane ordering. Besides the bulk Bragg peaks at *l* equals −5,−2, 1, and 4, smaller but significant peaks are found at *l* values of exactly −4,−1, 2, and 5. These peaks correspond to twinned InP islands on the surface with a surface coverage of about 5%. Important to note is that these twinned features are absent before heating and appeared during the measurements after roughly one hour at elevated temperature. The twin peaks become more pronounced in time, but during the total data collection never covered more than 10% of the surface.[30]

By comparing the CTR from bulk-terminated InP (black line) with the measured data (red triangles), we find that at *l* values around +3 and −3 that there are clear systematic deviations. Around $l = 3$, the scattered intensity is somewhat lower than what would be expected, and around $l = -3$ it is somewhat higher. The deviations indicate that some degree of in-plane ordering is present in the first layer of the liquid. From fitting, we find that only the first layer shows such ordering. If all the atoms in the quasi-liquid layer would show strong in-plane ordering, the (1,0,*l*) rod should, just as the specular one, also show a broad diffraction feature, which is absent. The other layers can therefore be described using an "infinitely" large in-plane Debye−Waller parameter.

If we now consider in-plane ordering of the first layer in the metal alloy, the atoms can be located at three positions on top of the zinc-blende substrate. They can be on top of the P atoms (continued zinc-blende bulk structure), on top of the In atoms, or at the hollow site at the center of the hexagonal InP rings, indicated in Figure 3a. Two model calculations are shown in Figure 2 with the first layer at the hollow site (green) and zinc-blende position (blue). By comparing the calculated rod profiles for these stacking possibilities, we find that the asymmetry is reproduced only by placing the atom in the first layer of the quasi-liquid at the hollow site. The atoms are thus preferentially located in the center of the hexagonal rings, as shown in Figure 3c. When nucleating the next crystalline bilayer, In will always be positioned on top of the P atoms of the previous bilayer. Only the P atoms in the new layer will determine the stacking. There are two possibilities, either continuing the zinc-blende structure or forming a stacking fault, corresponding to the start of the wurzite structure. Because we find that the hollow sites are preferentially occupied by Au/In alloy atoms, the P atoms will be sterically hindered to enter the zinc-blende positions and are therefore stimulated to crystallize in the wurzite structure.

The data presented here indicate that close to the interface a strong ordering occurs in the *z*-direction, manifested by layering, as well as preferential in-plane ordering. The formation of a quasi-liquid on top of the substrate surface will have a major impact on the growth behavior. At the free surface of SiAu alloys close to their eutectic composition, even a layering of seven layers is found,[16,32] which is accompanied by the formation of a solid 2D surface alloy. It could be that the driving force, which is responsible for the crystallization of the alloy layer at temperatures close to the eutectic point, induces the strong layering. Because of the strong layering, we argue that the growth mechanism is more complex than simply VLS, and in principle should be described by a "vapor−quasiliquid−solid (VQLS)" growth. Interfacial ordering is expected to have a large influence on the crystal growth, most notably on the growth rate. For other materials systems, the alloy compositions could have a different preordering at the growth interface and possibly lead to other preferential crystal structures. This could be the case for GaP, which exhibits the zinc-blende crystal structure for nanowires grown by a AuGa alloy[12,15] which is the same as for bulk-grown crystals.

In summary, we have shown that the first three atomic layers of the liquid AuIn metal alloy are strongly layered and

DOI: 10.1021/nl1023996 | *Nano Lett.* **2011,** *11,* 44–48

that the first of these atomic layers shows in-plane ordering with the periodicity of the underlying substrate. This quasi-liquid structure will have clear consequences for the mass transport during nanowire growth at this interface. The first layer, closest to the P-terminated InP substrate interface, is likely an In rich layer and contains approximately 70% In, compared to 40% in the bulk of the liquid. From the in-plane ordering, we find evidence for a preferential positioning of the first atomic layer at hollow sites, which sterically hinders the formation of a zinc-blende structure and thus leads to wurtzite InP nanowires.

Acknowledgment. We thank L.F. Feiner for valuable discussions. This research was carried out under Project Number MC3.05243 in the framework of the strategic research program of the Materials innovation institute (M2i) (www.M2i.nl), the FP6 NODE (015783) project, the ministry of economic affairs in The Netherlands (NanoNed), and the European Marie Curie program. The authors would like to thank E. van Thiel for the deposition of metal alloys, H. Wondergem for ex-situ XRD measurements, and H. de Barse for SEM imaging.

REFERENCES AND NOTES

(1) Wagner, R.; Ellis, W. Vapor-Liquid-Solid mechanism of single crystal growth. *Appl. Phys. Lett.* **1964**, *4*, 89–90.
(2) Verheijen, M. A.; Immink, G.; de Smet, T.; Borgstrom, M. T.; Bakkers, E. P. A. M. Growth Kinetics of Heterostructured GaP-GaAs Nanowires. *J. Am. Chem. Soc.* **2006**, *128*, 1353–1359.
(3) Joyce, H.; Wong-Leung, J.; Gao, Q.; Tan, H.; Jagadish, C. Phase Perfection in Zinc Blende and Wurtzite III-V Nanowires Using Basic Growth Parameters. *Nano Lett.* **2010**, *10*, 908–915.
(4) Algra, R.; Verheijen, M.; Borgström, M.; Feiner, L.; Immink, G.; van Enckevort, W.; Vlieg, E.; Bakkers, E. Twinning superlattices in indium phosphide nanowires. *Nature* **2008**, *456*, 369–372.
(5) Glas, F.; Harmand, J.; Patriarche, G. Why does Wurtzite form in nanowires of III-V Zinc Blende semiconductors? *Phys. Rev. Lett.* **2007**, *99*, 146101.
(6) Tabuchi, M.; Ohtake, A. M. Y.; Takeda, Y. X-ray CTR scattering measurement to investigate the formation process of InP/GaInAs interface. *J. Phys.: Conf. Ser.* **2007**, *83*, No. 012031.
(7) Sorensen, B. S.; Aagesen, M.; Sorensen, C. B.; Lindelof, P. E.; Martinez, K. L.; Nygård, J. Ambipolar transistor behavior in p-doped InAs nanowires grown by molecular beam epitaxy. *Appl. Phys. Lett.* **2008**, *92*, No. 012119.
(8) Kodambaka, S.; Tersoff, J.; Reuter, M. C.; Ross, F. M. Germanium Nanowire Growth Below the Eutectic Temperature. *Science* **2007**, *316*, 720–732.
(9) *Phase Equilibria, Crystallographic and Thermodynamic Data of Binary Alloys*, vol. IV/5a of Landolt-Bornstein New Series. Springer, 1991.
(10) Dick, K.; Kodambaka, S.; Reuter, M.; Deppert, K.; Samuelson, L.; Seifert, W.; Wallenberg, L.; Ross, F. The Morphology of Axial and Branched Nanowire Heterostructures. *Nano Lett.* **2007**, *7*, 1817–1822.
(11) Bakkers, E.; Verheijen, M. A. Synthesis of InP nanotubes. *J. Am. Chem. Soc.* **2003**, 3440.
(12) Verheijen, M.; Algra, R.; Borgström, M.; Immink, G.; Sourty, E.; van Enckevort, W.; Vlieg, E.; Bakkers, E. Three dimensional morphology of GaP-GaAs nanowires revealed by transmission electron microscopy tomography. *Nano Lett.* **2007**, *7*, 3051–3055.
(13) Dick, K.; Kodambaka, S.; Reuter, M.; Deppert, K.; Samuelson, L.; Seifert, W.; Wallenberg, L.; Ross, F. The morphology of axial and branched nanowires hetereostructures. *Nano Lett.* **2007**, *7*, 1817.
(14) Borgström, M.; Immink, G.; Ketelaars, B.; Algra, R.; Bakkers, E. Synergetic nanowire growth. *Nat. Nanotechnol.* **2007**, *2*, 541–544.
(15) Johansson, J.; Karlsson, L. S.; Patrik, C.; Svensson, T.; Mårtensson, T.; Wacaser, B. A.; Deppert, K.; Samuelson, L.; Seifert, W. Structural properties of $(111)_B$-oriented III-V nanowires. *Nat. Mater.* **2006**, *5*, 574–580.
(16) Schülli, T.; Daudin, R.; Renaud, G.; Vaysset, A.; Geaymond, O.; Pasturel, A. Substrate-enhanced supercooling in AuSi eutectic droplets. *Nature* **2010**, *464*, 1174–1177.
(17) Robinson, I. Crystal truncation rods and surface roughness. *Phys. Rev. B* **1986**, *33*, 38303836.
(18) Ferrer, S.; Comin, F. Surface diffraction beamline ESRF. *Rev. Sci. Instrum.* **1995**, *66*, 1674.
(19) Balmes, O.; Rijnand, R.; Wermeilleand, D.; Restaand, A.; Petitand, L.; Isernand, H.; Dufraneand, T.; Felici, R. The ID03 surface diffraction beamline for in-situ and real time x-ray investigations of catalytic reactions and surfaces. *Catal. Today* **2009**, *145*, 220–226.
(20) Reedijk, M.; Arsic, J.; Hollander, F.; de Vries, S.; Vlieg, E. Liquid order at the interface of KDP crystals with water: Evidence for icelike layers. *Phys. Rev. Lett.* **2003**, *90*, No. 066103.
(21) Vlieg, E. Integrated Intensities Using a Six-Circle Surface X-ray Diffractometer. *J. Appl. Crystallogr.* **1997**, *30*, 532–543.
(22) Vlieg, E. ROD: a program for surface X-ray crystallography. *J. Appl. Crystallogr.* **2000**, *401−405*, 33.
(23) Kaminski, D.; Radenovic, N.; Deij, M.; Enckevort, W. v.; Vlieg, E. pH-dependent liquid order at the solid-solution interface of KH_2PO_4 crystals. *Phys. Rev. B* **2005**, *72*, 245404.
(24) Arsic, J.; Kaminski, D.; Poodt, P.; Vlieg, E. Liquid ordering at the Brushite-{010}-water interface. *Phys. Rev. B* **2004**, *69*, 245406.
(25) Huisman, W.; Peters, J.; Zwanenburg, M.; de Vries, S.; Derry, T.; Abernathy, D.; van der Veen, J. Layering of a liquid metal in contact with a hard wall. *Nature* **1997**, *390*, 379–381.
(26) Kaplan, W.; Kauffmann, Y. Structural Order in Liquids Induced by Interfaces with Crystals. *Annu. Rev. Mater.* **2006**, *36*, 1–48.
(27) It is also known from temperature-dependent nanowire growth investigations that at temperatures lower than the 693 K reported here the growth velocities become as low as is expected for vapor−solid−solid (VSS) growth.[8]
(28) McClelland, M.; Sze, J. Surface tension and density measurements for indium and uranium using sessile-drop apparatus with glow discharge cleaning. *Surf. Sci.* **1995**, *330*, 313.
(29) Lee, J.; Nakamoto, M.; Tanaka, T. Thermodynamic study on the melting of nanometer-sized gold particles on graphite substrate. *J. Mat. Sci.* **2005**, *40*, 2167.
(30) For unknown reasons, recrystallization at the interface occurs, due to some kind of surface restructuring, leaving InP islands of which a fraction is twinned. Although these unwanted twinned InP islands could not be prevented and were present on all the samples investigated, their relatively low coverage (<10%) does not influence the data analysis strongly. Indeed, the Bragg reflections of these twinned islands are found to contribute significantly only in a confined region ($\Delta l \approx 0.5$) and do not influence the scattering further away along the CTRs. In the (0,0,*l*) specular reflection twinning is not observed, because the *z*-direction is not sensitive to in-plane rotational twins. The twinned islands are modeled by a two unit cell (six monolayers) high layer with a surface coverage of 5%.
(31) Mattila, M.; Hakkarainen, T.; Mulot, M.; Lipsanen, H. Crystalstructure-dependent photoluminescence from InP nanowires. *Nanotechnology* **2006**, *17*, 1580–1583.
(32) Shpyrko, O.; Streitel, R.; Balagurusamy, V.; Grigoriev, A.; Deutsch, M.; Ocko, B.; Meron, M.; Lin, B.; Pershan, P. Surface Crystallization in a Liquid AuSi Alloy. *Science* **2006**, *313*, 77.

DOI: 10.1021/nl1023996 | *Nano Lett.* **2011,** *11,* 44–48